Prospects and Challenges of Bremsstrahlung-based Electrostatic Potential and Material Composition Determination for Spacecraft

Kieran Wilson and Hanspeter Schaub

***Abstract*—Despite decades worth of data on spacecraft charging and its risk, measuring the charging on a nearby space object during close proximity, servicing and rendezvous and docking operations without requiring physical touch remains challenging. This work proposes a means to identify the charge on a closely neighboring space object and its elemental composition by examining the x-ray spectrum generated by energetic electrons impacting the target. In particular, deconvolution of the bremsstrahlung x-ray continuum provides an estimate of the landing energy of the electrons. Knowing the initial electron energy, the potential difference between the source and the target is determined. Additionally, characteristic x-rays emitted during the process of energetic electron-matter impact allows the relative abundance of elements in the target to be determined. Spatial separations on the order of 10s of meters are required between an electron gun and the corresponding detector to maximize collection of the bremsstrahlung spectrum. This could be achieved with either a single craft and deployable booms, or through the use of two spacecraft. Electron beam energies of 40 kV and currents of 1 miliamp are found to generate sufficient levels of x-rays for potential determination at over 10 meters from the target, and to determine the landing energy of the beam to within 0.14%.**

I. Introduction

Electrostatic charging has been a known consequence of spaceflight since the early days of space exploration. As spacecraft interact with the space environment they experience currents as a result of electron emission induced by the photoelectric effect of the sun's radiation, and through currents of electrons and ions in the space plasma [1]. Several experiments have sought to characterize the charging environment at geostationary orbit (GEO); notably SCATHA and ATS-6, missions which flew at geostationary orbits in the 1980s, demonstrated that spacecraft operating could charge to tens of kilovolts under certain conditions at GEO [2].

These missions also demonstrated the use of active charge control using electron or ion guns [3]. Whether natural or forced, spacecraft charging can create dangerous situations for spacecraft as differential charging can result in arcing and potential electronics damage. Differentially charged spacecraft components can lead to arcing hazards, a frequent cause of damage to solar panels [4]. Brandhorst and Rodiek found half of satellite insurance claims to be the result of solar panel anomalies, motivating a need to better understand charge distributions on spacecraft to mitigate such issues [5].

This threat also applies in rendezvous and servicing missions, as bodies charged to different potentials may experience damaging arcing as they contact [1]. In Low Earth Orbit (LEO), Carruth et al. determine that under certain conditions charge differentials could be significant enough to injure or kill astronauts performing extravehicular activities without proper mitigation [6].

However, thus far, it has only been possible to measure the potential on an instrumented craft itself. In many proposed missions to service, refuel or re-orbit spacecraft this would be insufficient information to prevent arcing. Such methods also cannot provide needed information for proposed missions which seek to harness electrostatics for touchless object manipulation, such as detumbling space debris or the electrostatic tractor concept for remotely re-orbiting debris away from operating geostationary satellites [7], [8]. Other missions have been proposed to utilize Coulomb forces to establish spacecraft constellations, enabling missions via fuelless formation flying that are impossible to do with monolithic spacecraft, and without plume impingement contamination and fuel consumption issues that come with traditional thrusters [9].

In addition to enabling a range of novel mission concepts, the ability to measure spacecraft potentials touchlessly in situ will contribute to the overall understanding of spacecraft charging, and lead to better methods for mitigating potentially hazardous charging conditions.

Prior work on charge sensing has largely focused on measuring a spacecraft's own charge, as an indicator of potentially dangerous charge situations which operators could take steps to mitigate. However, some methods have been proposed to measure the charge on a spacecraft or celestial object remotely.

Knowledge of the charge of one spacecraft at GEO is insufficient to determine the charge of even nearby objects, as demonstrated by Koons et al. using data from seven geostationary spacecraft equipped with charge sensors. They found no relation between the charge states of spacecraft separated by just 0.4 hours of local time (5.5° of longitude). Koons et al. also determined that for awareness of hazardous charging conditions or anomaly diagnosis the state of neighboring spacecraft was effectively irrelevant, further reinforcing the need for remote potential determination [10].

Several methods have been proposed to fill this gap and allow the remote determination of charge for spacecraft. Fer-

Kieran Wilson is a graduate research assistant at the University of Colorado at Boulder, (email: kieran.wilson@Colorado.edu)

Hanspeter Schaub is a Professor and Glenn L. Murphy Chair of Engineering at the University of Colorado at Boulder, (email: Hanspeter.Schaub@Colorado.edu)

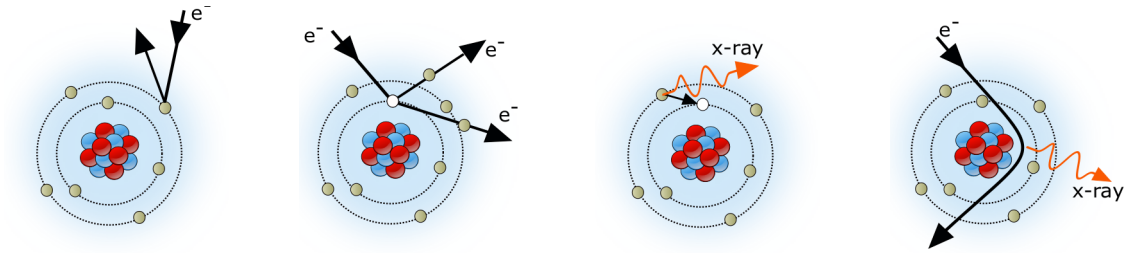

(a) backscattered electron

(b) Incoming electron knocking a secondary electron free of the atom

(c) An outer orbital electron dropping to fill the vacancy left by the secondary and releasing characteristic x-ray radiation

(d) An electron deflected by the positive charge of the nucleus and emitting a bremsstrahlung x-ray

Fig. 1. Four dominant interactions between energetic electrons and matter.

guson et. al propose a series of techniques that could provide remote indications of charging or arcing events on spacecraft, utilizing electromagnetic radiation including surface glows, bremsstrahlung x-rays, and radio or optical emission from arcing [11] to provide a measure of charge buildup. The authors conclude that detecting arcing events on GPS satellites may be possible from ground based radio telescopes, but other optical methods would require nearby spacecraft to determine when charging events occur. Additionally, the methods proposed cannot determine the level of charging occurring, but can sense only that it is happening.

Another approach provides an estimate of the voltage level based on secondary electrons generated in a material. Secondary electrons are emitted from atoms with near-zero initial energy, so determining the energy they arrive at a collector with allows the potential difference between the source and the collector to be determined. Halekas et al. demonstrated this concept with data from the Lunar Prospector mission to determine the charge of the Moon's surface during solar energetic particle events [12]. This method requires an electron detector positively biased relative to the surface being investigated to collect ejected electrons.

Using the evolution of relative position and velocity measurements between two spacecraft over time due to the Coulomb force, Bennett proposes a method for inferring the overall charge on a target craft [13]. This method has limitations associated with temporal resolution (requiring minutes to update the estimate of charge), charge resolution (which will be affected by accuracy of gravitational models and models of relative motion) and spatial resolution (only the total charge can be determined, as an effective sphere model).

An alternative method for close proximity charge determination is presented by Engwerda who proposes to measure the electric field around an object, and from there estimate the voltage and generate a multi-sphere model of charge distribution on the object [14], [15]. This work does not consider the difficulties associated with accurately measuring electric fields in an active charging scenario, nor in the sparse, hot plasma found at GEO. Further, this preliminary study makes the strong assumption of planar relative motion with a known trajectory.

Another category of remote charge sensing involves analyzing the electromagnetic radiation released when energetic particles impact a charged object. For instance, Lamoureux and Charles consider means of determining the landing energy characteristics of an electron population based on observations of the resultant x-ray spectrum. They present deconvolution schemes for monoenergetic beams as well as different plasmas, providing a baseline mechanism for extracting landing energy from an x-ray spectrum [16].

This x-ray spectrum also contains peaks which can be used to determine the elemental composition of a material. This has been applied in spaceflight previously, and is used by the REXIS instrument aboard Osiris-Rex to map elemental distribution across the surface of the asteroid Bennu. Instead of using energetic electrons to generate x-rays, REXIS relies on the characteristic x-ray fluorescence caused by solar x-ray excitation of the asteroid's surface [17].

This paper studies the use of an electron gun to charge the primary spacecraft positively, and target the electron emission onto the neighboring space object. The resulting bremsstrahlung x-rays provide a method to measure both local potential and material properties. The challenge is to determine what beam energies are required to create a strong enough return, how to measure the return signal, and to what accuracy the charge could be sensed. The novelty of this work is that is allows for charge sensing on a neighboring spacecraft or space object without physical touch. Further, in contrast to measuring secondary electron emission or inferring charge level from the perturbed relative motion, the x-ray based technique is able to perform high spatial resolution component charge and material property measurements within the space object structure.

The paper is organized as follows. First the bremsstrahlung-based charge sensing method is discussed, as well as the physics and challenges associated with characteristic radiation and the bremsstrahlung effect itself. Next the numerical modeling of Bremsstrahlung is described which allows for a numerical study of the electron landing energies and the resulting characteristic radiation. Implementation challenges such as sensor considerations, power and mass are discussed to evaluate the feasibility of this concept.

II. Sensing Method Overview

The method of material composition and potential determination studied in this paper is reliant on the use of an electron beam to generate x-rays from the target. Many complex phenomena occur when an electron beam impacts the material surface, as shown in Fig. 1. Bremsstrahlung x-ray generation is related to the landing energy of the electrons when they reach the material, which is a function of the voltage of the material and the energy of the electron beam. By measuring the x-ray emission and knowing the energy of the electron beam, the voltage of the material can be determined. The x-rays emitted by electron state changes, known as characteristic x-rays, are another product of this interaction and can additionally be used to determine the elemental composition of the target. An implementation of this concept to determine the surface charge and material composition of a defunct spacecraft is shown in Fig. 2. Because the majority of the generated X rays are emitted in the direction of the beam, a second spacecraft or long boom may be needed to place the X ray detector where it can get the strongest signal.

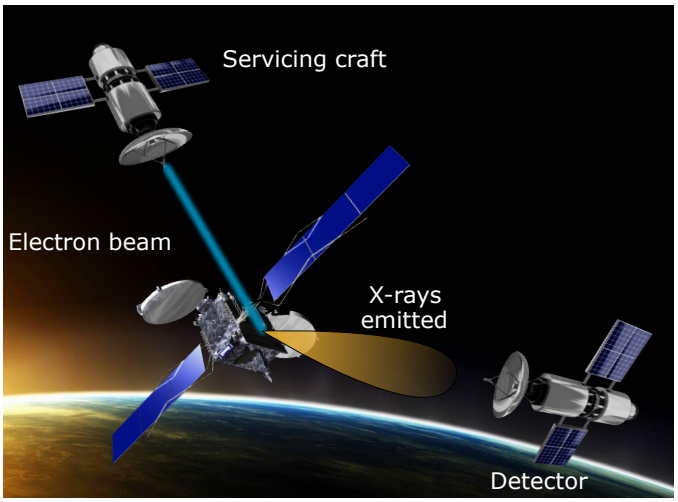

Fig. 2. Concept of operations for a 2 craft sensing configuration, where one uses an electron beam to generate x-rays, which are collected by a second craft.

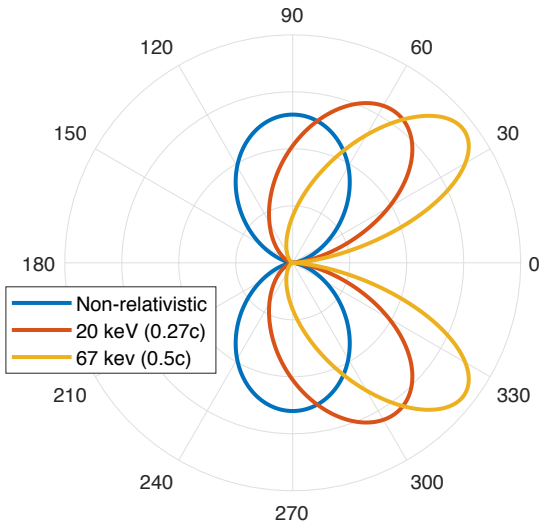

Fig. 3. Angles of bremsstrahlung emission as a function of incident electron energy. The electron is approaching from the left and interacting with an atom at the origin

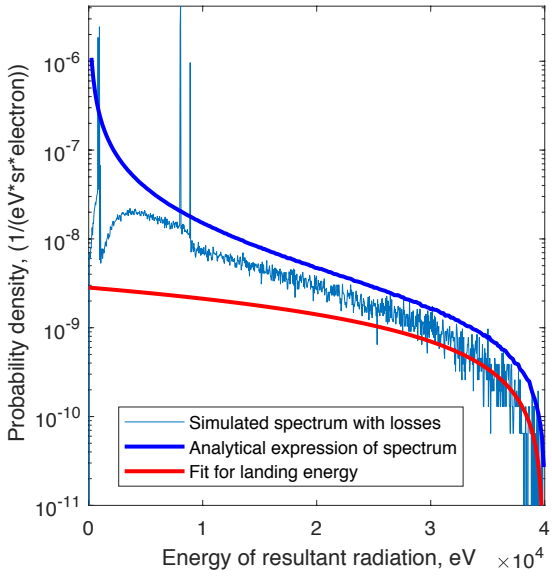

Fig. 4. Resultant x-ray spectrum illustrating both the bremsstrahlung continuum and the sharp peaks of characteristic x-ray emission.

III. Bremsstrahlung Description

As the electrons approach a material, they are subject to accelerations as a result of the voltage of the material either attracting or repelling the electrons. When the electrons collide with the atoms in the material, they slow down and release energy as electrons. Because the electrons will slow down by different amounts depending on their exact trajectory in the vicinity of the atomic nucleus this results in a continuous energy spectrum. This continuous energy spectrum is predominantly in x-ray energies, and is known as *bremsstrahlung* (German for "braking radiation") [18]. The highest energy photons that can be released by this process result from the case where an incoming electron is completely stopped by an atom, releasing its full kinetic energy as a single x-ray. The wavelength of such a photon is given by the Duane-Hunt law, as

$$\lambda_{\min} = \frac{hc}{eV} \tag{1}$$

where h is Plank's constant, c is the speed of light, e is the electron charge and V is the accelerating potential [18]. Therefore, a defined upper limit for photon energy is equal to the energy of incident electron; electrons with a landing energy of 40 keV will generate a bremsstrahlung spectrum with a maximum energy cutoff of 40 keV.

A. Angular distributions

The angle of emission of bremsstrahlung radiation is dependent on the energy of the incident electron; to a first

approximation, the power radiated as a function of angle can be related to incident electron beam energy by

$$P(\theta) \propto \frac{\sin^2(\theta)}{(1-\beta\cos(\theta))^5} \tag{2}$$

where θ is the angle relative to the electron beam, and $\beta = {}^{v_{\text{electron}}}/_{c}$ with c taken as the speed of light [19]. This relation is illustrated in Fig. 3 for three incident electron energies.

While this is a fairly simplistic approximation, it serves primarily to understand the underlying trends. As seen in Fig. 4, increasing the energy of the electron beam results in increasingly forward-directed photons. At non-relativistic velocities the primary radiation direction is nearly orthogonal to the incident beam; however, for 20 keV electrons the peak angle of radiation emission is 125° from the incident electron beam. This trend continues for higher energies, with MeV level electrons emitting photons predominantly in the forward direction. Increasing the landing energy has the effect of increasing the total energy radiated in proportion to E_0^2 while the output becomes more highly directed, effects that combine to improve numbers of photons detected at the optimal position.

The bremsstrahlung spectrum is doubly differential, in angle and in intensity. As the angle of the observer relative to the incident electron beam varies, the observed energy spectrum will vary as well. More accurate models exist, with the Koch and Motz 2BN model considered to be accurate to within 10% for the range under consideration in this work [20]. Therefore, this model is used for later analysis of photon fluxes at specific angles.

B. Radiation yield

Yield is described as an efficiency term, comparing energy deposited by the electrons to energy radiated by photons. One description developed by Kulenkopff proposes the efficiency to be a function of energy and atomic number of the target material of the form

$$\varepsilon = aZ(V_0 + 16.3Z) \tag{3}$$

where a is an empirically derived constant found to be 1.2×10^{-9} and V_0 is the potential the electron was accelerated through [19]. This efficiency term is therefore proportional to Z^2 and the incident electron energy; for 40 keV electrons interacting with aluminum, $\varepsilon = 0.06\%$, while the same electrons hitting gold would have an efficiency of $\varepsilon = 0.39\%$. This relation can be seen in Fig. 5.

The fraction of incident beam energy that is emitted as bremsstrahlung radiation is proportional to the incident beam energy, and to the square of the atomic number of the material Z [18]. Average yields for typical spacecraft materials such as aluminum or Kapton are assumed to be on the order of 0.01-0.1% for the energies under consideration here (up to 50 keV), increasing to closer to 1% for high mass elements like gold.

X-rays generated near the surface of a sample have a greater likelihood of escaping, rather than being absorbed by another atom [21]. Additionally, the forward directional nature of energetic bremsstrahlung radiation seen in Fig. 3

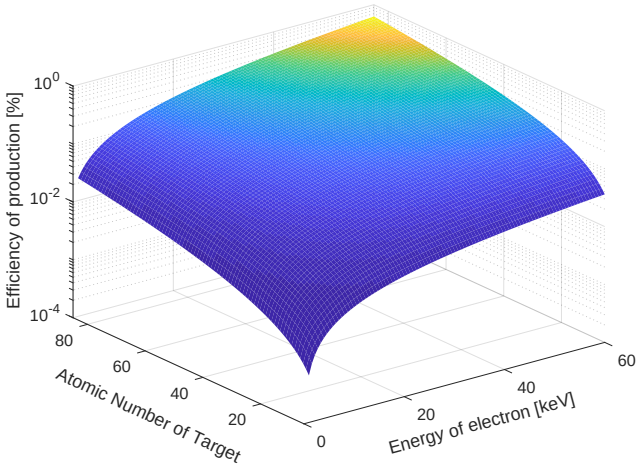

Fig. 5. Radiation yield as a function of atomic number of the target and incident energy of the electron. The maximum yield in the figure is 0.64%.

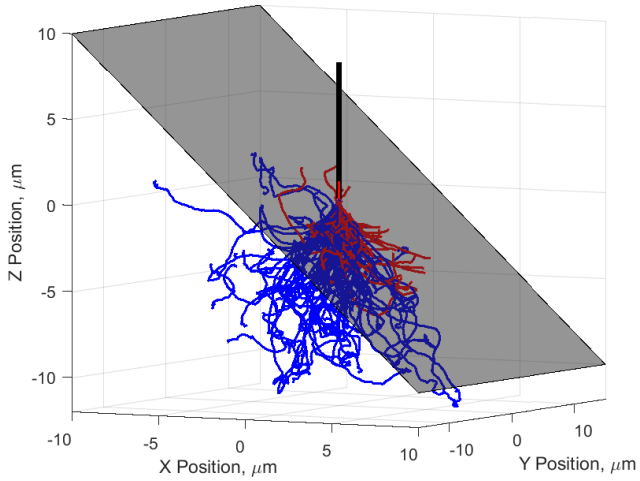

Fig. 6. 40 keV electron trajectories through an aluminum target. Red trajectories indicate electrons which have escaped the material; blue paths indicate those which were absorbed. The material boundary is indicated by the grey surface; the thick black line is the incident electron beam originating in the +Z direction.

means that a highly inclined target, where a greater fraction of the interactions take place near the surface and there is less material in the direction of the bremsstrahlung emission lobe, is favorable for x-ray detection. Fig. 6 illustrates the path of an electron shower in an inclined aluminum target. At each interaction, the electrons lose energy either through ionization of the impacted atom or through bremsstrahlung radiation. Target self-absorption of the generated x-rays is less significant for a surface that is highly inclined relative to the incident electron beam than for one that is near perpendicular, due to the forward directional bias of bremsstrahlung [18]. Therefore, a higher fraction of generated x-rays will escape the target and create a scenario more favorable to detection of the x-rays.

IV. Modeling of x-ray emission

A wide range of factors affect the x-ray spectrum at a given point, including incident electron beam energy, angle between the beam and the detector, and the target material. To gain insight into this process, several of these aspects are analyzed using fairly simple approximations, and the final results confirmed using sophisticated Monte Carlo based modeling codes.

Bremsstrahlung can be subdivided by various categories which affect the methods available to analyze and simulate it. One of the most significant describes the nature of the target, as either a thin or thick sample. "Thin" refers to a specimen in which an incident electron is likely to have only one interaction with an atom before being transmitted; in this case, there is little absorption of the generated radiation by the sample and the electrons all have the same initial energy prior to their interaction. "Thick" targets, meanwhile, have a large fraction of the incident electrons absorbed by the target after a series of energy-shedding interactions, and are the subject of analysis here. Because electrons interact with a large number of atoms as they lose energy, the resultant bremsstrahlung spectrum is distinctly different from that generated by thin-target interactions [16]. Additionally, the surrounding atoms absorb some of the bremsstrahlung x-rays before they can be emitted outside of the target; low-energy photons are particularly susceptible to absorption, depressing the number of photons emitted in higher wavelength parts of the spectrum as seen in Fig. 4 [19], [21].

Bremsstrahlung can arise as a result of an energetic electron accelerating in the vicinity of an atom, or by undergoing polarization in an electron cloud. Polarizational bremsstrahlung is a fairly small effect relative to atomic for the problem under consideration here, so the focus in this work will be on atomic, or classical, bremsstrahlung [19].

Incident electron energies of interest are likely to be in the region of 10-60 keV, based on an anticipated beam energy of 30-40 kV and a potential difference to the target of up to 20 kV. This range is in the realm of mildly relativistic electrons, where relativistic effects cannot be ignored but neither are high energy approximations appropriate (a 10 keV electron has $\beta = v/c = 0.195$ while 60 keV is $\beta = 0.446$). Therefore, the problem of interest can be narrowed to the generation of x-rays in a thick target by mildly relativistic electrons, a problem which is well described by the Koch and Motz 2BN model discussed earlier [20]. In addition to the analytic implementation described previously, this model is integrated into the pyPENELOPE Monte Carlo framework for simulating electron-matter interaction. Simulation of the bremsstrahlung spectrum was performed mainly in pyPenelepe, an open-source Python-based framework for the widely-used PENELOPE Monte Carlo codes. Penelope makes use of a variety of methods for simulating the coupled electron-photon transport and formation [22]. This code was used to generate simulated bremsstrahlung spectra shown in Fig. 4, as well as the electron trajectories in Fig. 6.

A. Spectral distribution

The bremsstrahlung spectrum has a maximum cutoff energy, discussed earlier in equation (1). Additionally, due to self-absorption of longer wavelengths by surrounding atoms, the flux is expected to decay to zero as the energy approaches zero, as seen in Fig. 4.

Empirical models exist to describe the thick target bremsstrahlung distribution, such as that of Kulenkampff, which is agnostic to how relativistic the incident electrons are [19]. This model is used to generate the spectra at three energies in Fig. 3.

A basic model of the energy spectrum is provided by Kramer's Law, which can be written as

$$I(\lambda)d\lambda = \frac{K}{\lambda^2}\left(\frac{\lambda}{\lambda_{\text{max}}} - 1\right) \tag{4}$$

where K is a constant that varies proportionally with the atomic number of the target element, typically written as Z [19].

This model is a reasonable starting approximation, but fails to account for absorption of the x-rays by the target material or electron backscattering, effects which can be quite significant for thick targets. Analytic modifications have been proposed to improve the accuracy of the model for thick targets, most notably by Brunetto [23]. The Koch and Motz 2BN model is accurate to within 10% for the energy range under consideration here, and is the most accurate analytic model available for mildly relativistic thick-target bremsstrahlung. This model provides the analytic curve (in blue) shown along with a simulation of the detected spectrum in Fig. 4.

B. Landing energy determination

The simplest approach to determining the electron landing energy would be to determine the maximum x-ray energy detected. As discussed earlier, this maximum x-ray energy is equivalent to the case where the electron is fully stopped and its full landing energy is converted to an x-ray with a magnitude in the limit of the Duane-Hunt law in equation (1).

However, several issues are raised by this method. First, the sun emits significant quantities of hard x-rays, so any small quantity of high energy x-rays could be the product of bremsstrahlung at the site by the electron beam or of solar emissions, or even the result of high energy electrons in the ambient plasma creating bremsstrahlung interactions. Additionally, the number of electrons which are fully stopped in one collision is vanishingly small, and the chance of detecting such an x-ray in a realistic scenario with a small detector far from the origin is smaller still. Therefore, very long collection times would be required to have a significant sample near the very limit of the energy range, and would require no solar x-ray interference and sophisticated filtering of sensor noise.

Alternatively, Lameroux and Charles propose a more robust method for determining the landing energy of the electrons via deconvolution of the bremsstrahlung spectrum. For a spectrum resulting from a monoenergetic incident electron beam, a linear fit to the high energy portion of the spectrum (where

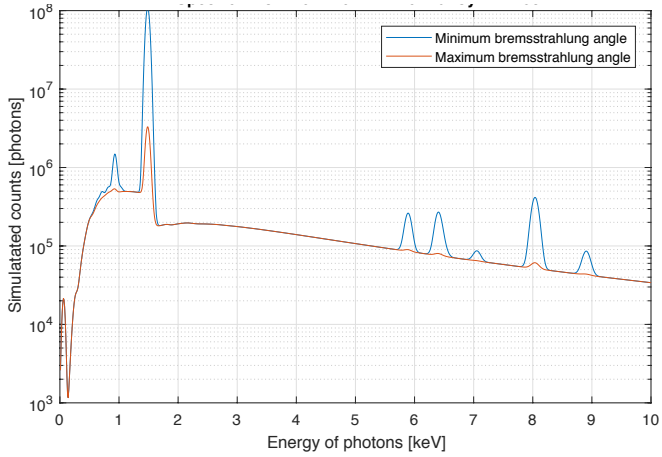

Fig. 7. Near maximum and minimum bremsstrahlung spectra, normalized by magnitude of the spectrum to allow for comparison between the relative magnitude of the characteristic spike and the continuum spectrum.

$E > 0.9E_0$) is recommended [16]. This line has the landing energy of the electron beam as its x-intercept, allowing a straight forward means of determining the landing energy, as shown by the red line in Fig. 4.

V. Characteristic Radiation

The bremsstrahlung continuum provides a means of identifying the electrostatic potential of a surface. However, the characteristic radiation emitted through electron-matter interaction can provide another important assessment of a surface: the elemental composition.

In addition to the bremsstrahlung continuum radiation, characteristic radiation is emitted as a byproduct of ionization interactions in the target material. When the incident electron excites an inner-shell electron in the target material to ejection, the resulting vacancy is filled by an outer shell electron. This electron releases a photon as it drops with energy equal to the difference in energy of the two shells. Because this energy difference is specific to the atom, the radiation can be used to identify the element. The energy difference between the two shells is emitted as a photon, the energy of which can be used to determine the electron transition and element it originated from. While these photons are emitted isotropically, spectroscopy for elemental identification of the target is easier in areas away from the primary bremsstrahlung lobe to avoid masking the characteristic radiation signal, as seen in Fig. 7.

The characteristic spikes can be observed in Figs. 4 and 7, as the sharp peaks in the simulated x-ray spectrum. Each peak corresponds to an electronic transition, as a valence (outer level) electron falls to a lower energy state to fill a vacancy formed when an inner electron is ejected by an impacting electron.

These peaks allow the material to be identified as copper in Fig. 4, while Fig. 7 shows the spectrum resulting from Al2195, an aluminum-lithium alloy commonly used in spacecraft and rocket bodies [24]. From this spectrum, it is relatively straightforward to identify aluminum as the dominant element, based on the relative level of the peaks; the relative concentrations of the alloying elements (lithium, copper, silver and magnesium) can be determined by a similar process.

An open source program developed by NIST for energy dispersive x-ray spectroscopy, DTSA-II, was used to simulate and analyze the characteristic spectra generated, and was used to generate the curves in Fig. 7 [25]. It is worth noting that while the complete set of peaks is unique to a specific element, some transitions can be very similar between elements, complicating identification [25], [18].

While the characteristic peaks provide a useful means of determining a surface's composition, many spacecraft make use of aluminized Mylar or Kapton for thermal control, often as part of multilayer insulation (MLI). While coated in a metal, MLI is primarily composed of dielectric materials, which could lead to false conclusions about the charge capacity and conductivity of sections of the craft. However, from Fig. 6, 40 keV electrons penetrate up to 10 μm into a material. For comparison, typical metallic coatings used for thermoregulation of spacecraft are on the order of 0.1 μm in thickness. Therefore, even if a surface is covered in a layer of gold or aluminum, the substrate material can still be identified via characteristic radiation generated by the penetrating electrons [26].

VI. Implementation

When considering how the system discussed could be implemented in the real world, several significant factors must be addressed. Defunct spacecraft in GEO frequently have high rotational rates, up to 10s of degrees per second [27]. Because of the risk of a collision, separation distances between the target and the servicing craft of at least the radius of the craft are desired, taken here to be on the order of 10 meters. Additionally, sensors must be selected with sufficient resolution and detector area to provide an accurate assessment of material composition and surface potential. Finally, the components of the system must be capable of performing in the space environment.

A. Boom vs two craft

First, the forward-directional nature of bremsstrahlung poses spatial constraints due to the separation required between the detector and the electron source. As discussed earlier and illustrated in Fig. 3, bremsstrahlung emission peak emission direction is a function primarily of incident electron energy. For an electron beam with a 10 keV landing energy, the direction of peak emission is 115.6° from the direction of the beam source; for a 60 keV beam, the angle will be 142°, per the Koch and Motz 2BN model.

Assuming a standoff distance of 10 meters, even a 10 keV beam (which has a relatively small x-ray emission angle) would require over 20 meters of separation between the beam source and the x-ray detector, a challenging distance to achieve with one craft. Furthermore, 10 meters is likely to be at the lower end of acceptable distances to tumbling multi-ton spacecraft, necessitating further distances with larger separations. Likewise, the increasing separation distance required by increasing landing energies and changing direction of peak emission suggests that this would be best approached as a

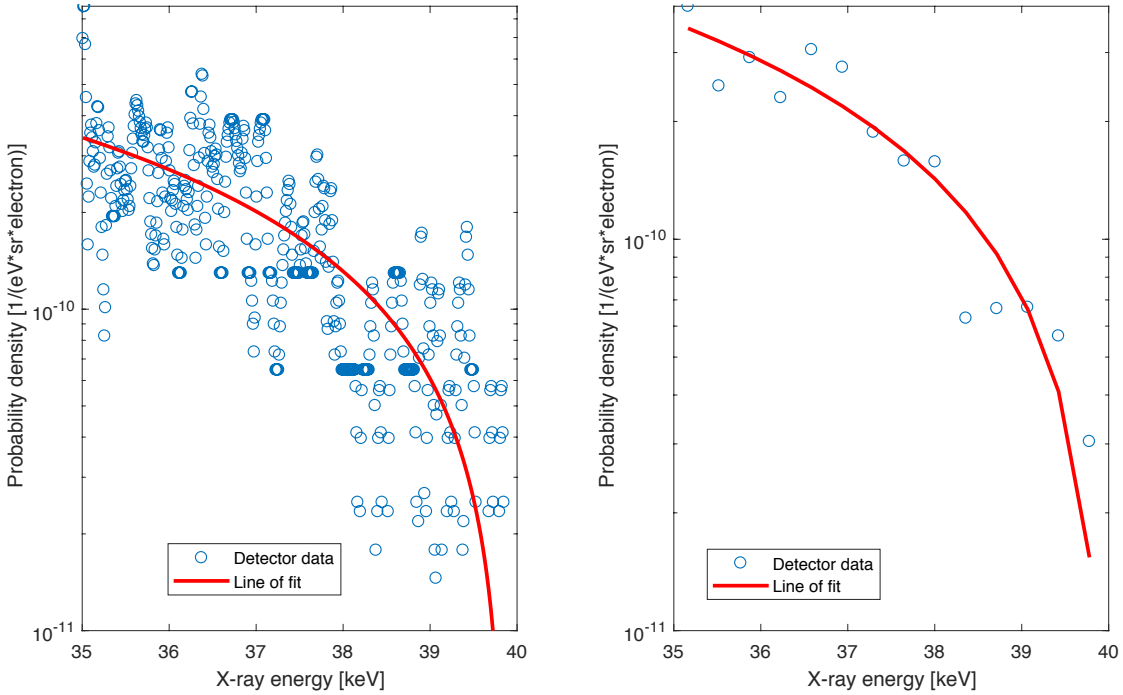

(a) High energy spectrum with 10 eV resolution

(b) High energy spectrum with 355 eV resolution

Fig. 8. High energy part of spectrum (>35keV) simulated with detector resolutions of 10 and 365 eV. The computed landing energies in each case have errors of 136 and 6 eV, respectively.

formation flying problem, with separate craft carrying the electron gun and the x-ray detector. This solution would also enable new approaches to prior proposed electrostatic actuation of uncontrolled craft, potentially allowing improvements in performance over detumbling and re-orbiting scenarios that have been previously explored [13].

However, a boom-based solution utilizing only one craft may still be functional for certain missions, and the limitations of this approach are the subject of future work. No requirements are placed on the location of the sensor relative to the detector for characteristic radiation detection. Booms have previously been developed and flow with lengths of over 100 meters, though these systems have a fixed deployed length [28]. Such a design could potentially be adapted to support an x-ray spectrometer for sensing applications.

B. Sensor considerations

Any optical sensor is subject to noise and limits to the size of the detector, with larger detectors capable of receiving more photons and typically reduced levels of noise. Furthermore, x-ray detectors have efficiency curves as a function of energy, performing much better at some wavelengths than others. At low energies, this attenuation is typically the result of absorption by the detector window, while high energies typically interact less strongly with the sensor and may instead pass through and interact with material behind the sensor [29].

For this application, commercial versions of two sensor types (either higher resolution silicon drift detectors or lower resolution but larger Si-PIN detectors) could be implemented, with trade-offs between sensor resolution, related to accuracy of landing energy measurement, and size, which affects number of photons collected and therefore temporal resolution [30]. Temporal resolution is important as the electron gun operation will alter the charge of the target craft over time, so minimizing collection time can reduce the resultant perturbation of the object's charge. Additionally, for a tumbling target, improved temporal resolution will result in a higher fidelity model of the target's elemental composition and a better understanding of charge distribution on the target.

To analyze the dependence of the bremsstrahlung spectrum on angle and energy, the Koch and Motz 2BN model, an analytic expression optimized for low energy mildly relativistic electrons, was implemented in Matlab [20]. This expression provides the the shape and intensity of the spectrum at any angle to the incident electron beam.

Because of the deconvolution scheme used to determine the landing energy of the electrons is based on the trend of the high energy x-ray data, accuracy of the landing energy calculation is only somewhat related to the accuracy of the computed landing energy. This relationship is illustrated in Fig. 9. Despite a simulated detector resolution of 490 eV, this method was still able to determine the landing energy of the electrons in worst case sensor in Fig. 9 to within 54 eV, less than 0.14% total error. The under-performance of the ideal, fully sampled case is due to a high number of the high energy channels having detected no photons, as seen in Fig. 8.

Therefore, the sensor selection for potential determination can favor increasing detector size over resolution, two factors that are difficult to combine in a small device suitable for use

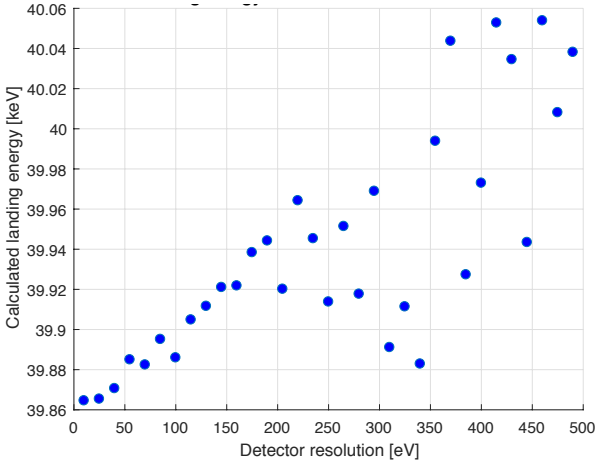

Fig. 9. Calculated landing energy as a function of detector resolution

on spacecraft. Spectrometer sensor size is critical to capturing as many x-rays from the high energy portion of the spectrum as possible to maximize accuracy of the landing energy determination. Because only 0.1% of the photons generated are in the range of $E > 0.9E_0$ and just 0.08% of electron kinetic energy is converted to photons, even a relatively large x-ray sensor of 25 mm^2 at a near 10 meters to the target will be hit by an energy flux of just 5×10^{-10} times the incident power of the electron beam. However, this still translates to a total of 3.5×10^6 photons per second in this high energy range, based on an assumed electron gun with a current of 1 milliamp and emission potential of 40 kV for a total power output of 40 watts.

Reducing the resolution of the sensor, however, will have a negative impact on resolving characteristic lines and therefore on the ability to determine material composition. Additionally, care must be taken to exclude solar radiation from the sensor, as trace amounts of heavy elements in the corona are energized to emit characteristic x-rays that could make determination of the target material more difficult [31].

C. Power and Mass

The addition of any system to a spacecraft is critically evaluated for impact to two scarce resources: power and mass. The booms described previously as a potential method for single-craft operation have masses of less than 12 kg for a 100 meter fixed-length boom, with no direct power impact after deployment [28]. A two craft system naturally has a higher power and mass impact than a system that can be integrated into only one spacecraft.

However, two craft may provide performance benefits in many servicing or electrostatic reorbiting applications, mitigating the overall mission impact.

X-ray detectors with flight heritage in the NEAR and Mars Pathfinder missions consume less than 1 Watt and have mass of less than 140g (based on the Amptek XR-100 detector) [30]. This would have a limited impact on most spacecraft missions.

High energy electron beams have been flown in space on prior missions. Notably, the EXOS-B and SCATHA satellites were equipped with electron guns up to 200 eV and 1 mA currents in near-GEO space. In suborbital sounding rocket experiments, far more powerful electron guns have been tested in space. The ECHO-2 experiment carried pulsed beam electron gun with 80 mA current and 45 keV voltage, on a similar scale to those proposed for use here [32].

Even higher energy systems have been studied for use in space; Eubert and Gilchrist propose flying a linear accelerator emitting electrons with energies up to 5 MeV, declaring the technology feasible for orbital applications [33].

VII. Conclusions

A system is proposed to determine the electrostatic potential and elemental composition of a space object from distances of greater than 10 meters. By using an electron gun with an energy of 40 kV and 1 milliamp, combined with an x-ray detector with a resolution of at least 400 eV, the landing energy of the electrons can be determined to sub 1% accuracy. All major elements of the system have some degree of flight heritage, improving the feasibility of this method. Additionally, this could enable future missions based on electrostatic actuation of debris or rendezvous and servicing, opening up new opportunities for utilizing the space environment.

Low earth orbital environments, specifically high densities of cold plasma, may make this method more difficult to implement due to uncertainty in the interaction of the electron beam with the ambient plasmas. This is an area for future study. Additional work is required to determine the impact of a two-craft formation compared to the results that could be achieved by a single craft with a boom-mounted detector.

References

[1] S. T. Lai, *Fundamentals of Spacecraft Charging: Spacecraft Interactions with Space Plasmas*. Princeton University Press, 2011.

[2] E. G. Mullen, M. S. Gussenhoven, D. A. Hardy, T. A. Aggson, and B. G. Ledley, "Scatha survey of high-voltage spacecraft charging in sunlight," *Journal of Geophysical Research*, vol. 91, no. A2, pp. 1474–1490, 1986.

[3] R. C. Olsen, "Experiments in charge control at geosynchronous orbit - ats-5 and ats-6," *Journal of Spacecraft and Rockets*, vol. 22, no. 3, pp. 254–264, May–June 1985.

[4] D. B. S. I. Katz, V. A. Davis, "Mechanism for spacecraft charging initiated destruction of solar arrays in geo."

[5] J. R. H. Brandhorst, "Improving space utilization by increasing solar array reliability," in *AIAA Space 2007*, 2007.

[6] R. S. M. M. M. R. Carruth, D. Ferguson, "Iss and space environment interactions without operating plasma contactor," NASA, Tech. Rep., 2001.

[7] T. Bennett and H. Schaub, "Touchless electrostatic three-dimensional detumbling of large axi-symmetric debris," *Journal of Astronautical Sciences*, vol. 62, no. 3, pp. 233–253, 2015.

[8] E. Hogan and H. Schaub, "Relative motion control for two-spacecraft electrostatic orbit corrections," *AIAA Journal of Guidance, Control, and Dynamics*, vol. 36, no. 1, pp. 240–249, Jan. – Feb. 2013.

[9] L. B. King, G. G. Parker, S. Deshmukh, and J.-H. Chong, "Spacecraft formation-flying using inter-vehicle coulomb forces," NASA/NIAC, Tech. Rep., January 2002.

[10] H. Koons, J. Mazur, A. Lopatin, D. Pitchford, A. Bogorad, and R. Herschitz, "Spatial and temporal correlation of spacecraft surface charging in geosynchronous orbit," *Journal of Spacecraft and Rockets*, vol. 43, no. 1, 2006.

[11] D. C. Ferguson, J. Murray-Krezan, D. A. Barton, J. R. Dennison, and S. A. Gregory, "Feasibility of detecting spacecraft charging and arcing by remote sensing," *Journal of Spacecraft and Rockets*, vol. 51, no. 6, 2014.

[12] J. Halekas, G. Delory, D. Brain, R. Lin, M. FIllingim, C. Lee, R. A. Mewaldt, T. Stubbs, W. Farrell, and M. Hudson, "Extreme lunar surface charging during solar energetic particle events," *Geophysical Research Letters*, vol. 34, no. 2, 2007.
[13] T. J. Bennett, "On-orbit 3-dimensional electrostatic detumble for generic spacecraft geometries," Ph.D. dissertation, University of Colorado Boulder, 2017.
[14] H. Engwerda, J. Hughes, and H. Schaub, "Remote sensing for planar electrostatic characterization using the multi-sphere method," in *Final Stardust Conference, ESTEC, The Nederlands*, Oct 2016.
[15] H. Engwerda, "Remote sensing for spatial electrostatic characterization using the multi-sphere method," Master's thesis, Delft University of Technology, Delft, The Netherlands, March 2017.
[16] P. C. M. Lamoureux, "General deconvolution of thin-target and thick-target bremsstrahlung spectra to determine electron energy distributions," *Radiation Physics and Chemistry*, vol. 75, no. 10, October 2006.
[17] R. A. Masterson, M. Chodas, L. Bayley, B. Allen, J. Hong, P. Biswas, C. McMenamin, K. Stout, E. Bokhour, H. Bralower, D. Carte, S. Chen, M. Jones, S. Kissel, M. S. F. Schmidt, G. Sondecker, L. F. Lim, D. S. Lauretta, J. E. Grindlay, and R. P. Binzel, "Regolith x-ray imaging spectrometer (rexis) aboard the osiris-rex asteroid sample return mission," *Space Science Reviews*, vol. 214, no. 48, February 2018.
[18] G. Pavlinsky, *Fundamentals of X-ray Physics*. Cambridge International Science Publishing, 2007.
[19] A. A. M. Rene E Van Grieken, Ed., *Handbook of X-Ray Spectrometry*, second edition ed. Marcel Dekker, Inc, 2002.
[20] H. Koch and J. W. Motz, "Bremsstrahlung cross-section formulas and related data," *Reviews of Modern Physics*, 1959.
[21] S. Morelhao, *Computer Simulation Tools for X-ray Analysis: Scattering and Diffraction Methods*. Springer International Switzerland, 2016, ch. Fundamentals of X-ray Physics.
[22] J. S. F. Salvat, J. M. Fernández-Varea, "Penelope 2006: A code system for monte carlo simulation of electron and photon transport." Nuclear Energy Agency Organisation For Economic Co-Operation And Development, 2006.
[23] M. Brunetto and J. Riveros, "A modification of kramer's law for the x-ray continuum from thick targets," *X-ray Spectrometry*, vol. 13, no. 2, 1984.
[24] "Super lightweight external tank," NASA Marshall Space Flight Center, Tech. Rep., 2005.
[25] N. Ritchie, "Efficient simulation of secondary fluorescence via nist dtsa-ii monte carlo," *Microscopy and Microanalysis*, vol. 23, no. 3, 2017.
[26] R. C. Langley, "Gold coatings for temperature control in space exploration," *Gold Bulletin*, vol. 4, no. 4, 1971.
[27] Y. S. Karavaev, R. M. Kopyatkevich, M. N. Mishina, G. S. Mishin, P. G. Papushev, and P. N. Shaburov, "The dynamic properties of rotation and optical characteristics of space debris at geostationary orbit," *Advances in the Astronautical Sciences*, vol. 119, 2004.
[28] "Helical quadrifilar coilable boom," Orbital ATK, Tech. Rep., 2005.
[29] C. R. Canizares, "Perspectives on high resolution x-ray spectroscopy," in *X-ray Spectroscopy Workshop*. MIT, 2007.
[30] "Xr-100cr si-pin x-ray detector," Amptek, Inc., Tech. Rep., 2018.
[31] K. Phillips, "The solar flare 3.8–10 kev x-ray spectrum," *The Astrophysical Journal*, 2004.
[32] J. R. Winckler, R. Arnoldy, and R. A. Hendrickson, "Echo 2: A study of electron beams injected into the highlatitude ionosphere from a large sounding rocket," *Journal of Geophysical Research (Space Physics)*, vol. 80, no. 16, 1975.
[33] B. G. T. Neubert, "Relativistic electron beam injection from spacecraft: performance and applications," *Advances in Space Research*, vol. 34, no. 11, 2004.